Parametric Design & Multi-Objective Optimization of Containerships

Alexandros Priftis[1], Apostolos Papanikolaou[2], Timoleon Plessas[2]

[1] Department of Naval Architecture, Ocean and Marine Engineering, University of Strathclyde, Glasgow, Scotland, Former National Technical University of Athens – Ship Design Laboratory, Athens, Greece
[2] National Technical University of Athens – Ship Design Laboratory, Athens, Greece

The introduction of the energy efficiency design index (EEDI) and ballast water treatment regulations by the International Maritime Organization, the fluctuation of fuel price levels, along with the continuous endeavor of the shipping industry for economic growth and profits has led the shipbuilding industry to explore new and cost-efficient designs for various types of merchant ships. In this respect, proper use of modern computer-aided design/computer-aided engineering systems (CAD/CAE) extends the design space, while generating competitive designs with innovative features in short lead time. The present article deals with the parametric design and optimization of containerships. The developed methodology, which is based on the CAESES/Friendship-Framework software system, is demonstrated by the conceptual design and multiobjective optimization of a midsized, 6500-TEU containership. The methodology includes a complete parametric model of ship's external and internal geometry and the development and coding of all models necessary for the determination of the design constraints and the design efficiency indicators, which are used for the evaluation of parametrically generated designs. Such indicators defining the objective functions of a multi-objective optimization problem are herein the EEDI, the required freight rate, ship's zero ballast container box capacity, and the ratio of the above to below deck number of containers. The set-up multiobjective optimization problem is solved by use of genetic algorithms and clear Pareto fronts are generated. Identified optimal design proves very competitive compared to standard container ship designs of the market.

KEY WORDS: parametric ship design; holistic optimization; containership

INTRODUCTION

Container Shipping Industry

Global containerized trade has been facing constant growth since 1996. In 2013, there was a 4.6% growth, which can be translated to a total movement of 160 million TEUs in 1 year (Clarkson Research Services 2014). The three routes on the major east–west tradeline—the transpacific, Asia–Europe, and the transatlantic—bring together the manufacturing center of the world, Asia, along with North America and Europe, which are considered to be the major consumption markets (UNCTAD 2014). In this project, the Asia–North America route is selected for the investigation of the required freight rate (RFR) in our model. It is worth mentioning that this particular route proved to be the most profitable in 2013, since 15,386,000 and 7,739,000 TEUs were shipped in its eastbound and westbound version, respectively (World Shipping Council, 2015). The Asia–North America route is served by most shipping companies and can be found in various versions. One of them is the India–North America route that is usually served by containerships in the 6000–7000 TEU category.

For a long time and until a few years ago, fuel prices were particularly high. However, since 2008, prices have dropped down and nowadays, heavy fuel oil (HFO) costs as low as 300 $/t. Marine diesel oil (MDO) has been following the same course and can be found at prices of around 500 $/t (PLATTS 2015). However, this does not always result in lower shipping rates. New international regulations regarding fuel emissions and the introduction of the so-called emission control areas (ECAs) have caused changes in the type of fuel used by ships. Carriers are now required to use low sulfur fuel in certain areas. As mentioned above, the difference in price between the types of fuel can be significant. In addition, the number of the ECAs is to be increased in the following years, which will broaden the use of the more expensive low sulfur fuel. Thus, it is imperative that cost-efficient designs are created, to overcome this encumbrance (Koutroukis 2012).

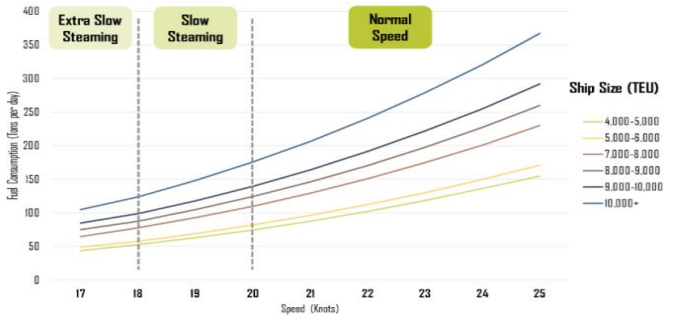

Fig. 1 Fuel consumption vs. speed (Notteboom & Carriou 2009)

Because of the increase of fuel prices, the shipping industry has adopted several practices to reduce fuel consumption. One of them is slow steaming (Fig. 1). Although some years ago containerships used to operate in speeds of around 25 knots, today this is no longer the case (Tozer 2008). Most container carriers operate in 18– 20 knots, to cut fuel costs. Along with the reduction in fuel consumption, vessels can achieve lower energy efficiency design index (EEDI) levels; hence, it seems that the trend of slow steaming is here to stay, even though fuel prices have slightly dropped recently (White 2010).

The recent improvement of technology and engineering made the introduction of ultralarge container vessels possible. A new trend, known as cascading, is the result of the high number of

new building programs initiated by many liner companies. These orders consist primarily of very large containerships. The continued influx of such large vessels into the market has led to a large number of vessels being cascaded onto tradelines that historically have been served by smaller vessels (Köpke et al. 2014). Hence, routes where 2000–3000 TEU containerships are preferred by charterers at the moment may attract larger vessels in the near future. Since the former category of ships is mainly used for the purpose of short sea shipping, ships in the 6000 TEU category could become widely popular among the shipowners and the charterers.

Although container carriers do not spend considerable amount of time in ports, port efficiency is one of the most important factors to be taken into account when designing a containership. The less the time spent in port, the more the time available for cruising at sea, which means that vessels can operate in lower speeds and consequently reduce fuel consumption. As a result, port efficiency is included in the optimization criteria of this study. Although complex and analytical simulations can be involved in a project dealing with port efficiency, in our case a more simple approach is followed, by monitoring the ratio of the above to below deck number of containers. It is obvious that the bigger the ratio, the faster the loading and unloading of containers; thus, the time spent by ships in port is reduced (Soultanias 2014).

State of International Regulations

We refer in the following to recent developments of international maritime regulations, which greatly affect future ship designs and herein particularly containerships.

Energy Efficiency Design Index In 2012, the International Maritime Organization (IMO) released guidelines on the method of calculation of the attained EEDI for new ships (Imo Resolution Mepc.212, 63, 2012). This is a major step forward in implementing energy efficiency regulations for ships, limiting fuel oil consumption and toxic gas emissions, through the introduction of the EEDI limits for various types of ships. The adopted EEDI measures became mandatory for new ships, whereas the introduced Ship Energy Efficiency Management Plan became a requirement for all ships, i.e., also for the existing ones, as of January 1, 2013. The EEDI relates the toxic gas emissions of a ship to her transportation work and is in fact an indicator of a vessel's energy efficiency. The determination of EEDI is based on a rather complicated looking (but indeed simple) formula, whereas it is required that the calculated value is below the level set by the IMO regulation for the specific ship type and size. The EEDI formula includes ship's fuel consumption and associated gas emissions in the nominator and ship's capacity and service speed in the denominator, with the product of the latter two values representing ship's transportation work. Clearly, the lower the EEDI, the more efficient is the ship, whereas ships are required to meet a minimum energy efficiency requirement set by the IMO regulation. The EEDI assesses the energy consumption of the vessel at calm water/sea trial conditions, while taking into account the energy required for propulsion and the auxiliary engines' hotel loads for the crew and passengers, if any. The formula considers corrections for increased fuel consumption in realistic sea conditions subject to proper evaluation of ship's powering in operating seaways. The EEDI requirement for new ships started with some baseline values in 2013, and is being lowered (thus becoming more stringent) successively in three steps until 2025, when the 2013 baseline values will have been reduced by 30%. It should be noted that there are serious concerns regarding the sufficiency of propulsion power and steering devices to maintain maneuverability of ships in adverse conditions, hence regarding the safety of ships, if the EEDI requirements are achieved by simply reducing the installed engine power of existing ship designs (IMO MEPC 64/4/13 2012). This refers especially to some ship types such as tankers and bulkcarriers, for which the initially set EEDI baselines are disputable. It is evident that EEDI is a rational, ship efficiency performance indicator that should be minimized in the frame of a ship design optimization.

Ballast Water Management The International Convention for the Control and Management of Ships' Ballast Water and Sediments was adopted in February 2004 by the IMO and applies to all ships, as of today. There are various approved technologies and systems currently available, dealing with ballast water treatment (BWT). All these aim at the minimization of the transfer of organisms through ballast water to different ecosystems, as the latter can cause serious environmental problems. However, the installation of such systems on both existing and new buildings increases the overall building and operational costs. Therefore, lately, research has been focusing at different solutions to reduce the amount of required ballast water, rather than effectively treating it by a proper BWT mechanism. The set problem is magnified for containerships, which inherently carry more ballast water, even at the design load condition, for which the ratio of the containers carried on deck to those carried under deck should be maximized. Thus, promising design solutions for modern containerships consider zero or minimal water ballast capacities. Nevertheless, attention should be paid to the overall cargo capacity as well, so as to maintain competitive values in all respects.

PARAMETRIC CAD MODELING OF SHIP DESIGN

In recent years, several authors have presented significant computer-aided design (CAD) methodologies dealing with the ship design process and inherently its optimization (Brown & Salcedo 2003; Campana et al. 2009; Mizine & Wintersteen 2010). A common characteristic of most of the earlier presented works is that they dealt with specific aspects of ship design (e.g., hydrodynamics, strength) or with new system approaches to the design process. The project presented herein deals with a fast, "holistic optimization" of a 6500-TEU containership, focusing on optimization of ship's arrangements, while considering all side effects on ship design, operation, and economy (Priftis 2015). This work complements two other related containership optimization studies of the National Technical University of Athens Ship Design Laboratory on the design of 8000 and 9000

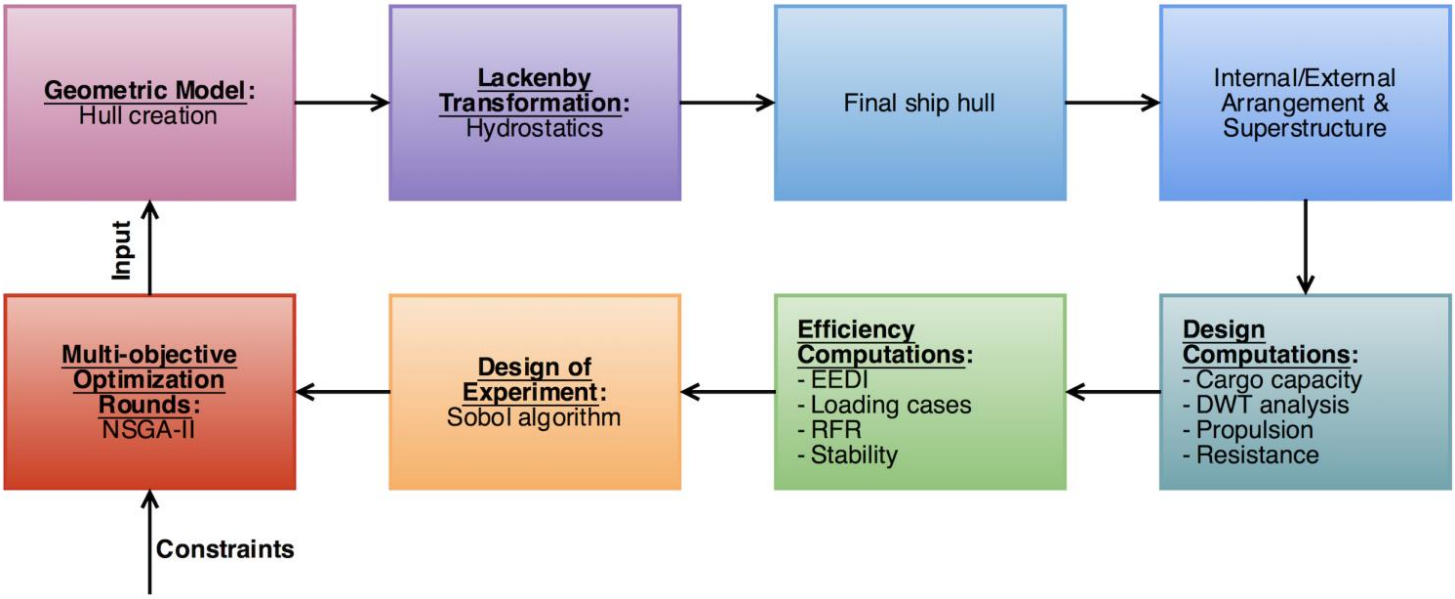

Fig. 2 Design optimization procedure

TEU (Koutroukis 2012; Soultanias 2014). "Holism" is interpreted as a multiobjective optimization of ship design and is based on the main idea that a system, along with its properties, should be viewed and optimized as a whole and not as a collection of parts (Papanikolaou 2010). Within this context, a parametric ship model of ship's external and internal geometry is created at first, followed by a multiobjective optimization to determine an optimal design (Fig. 2).

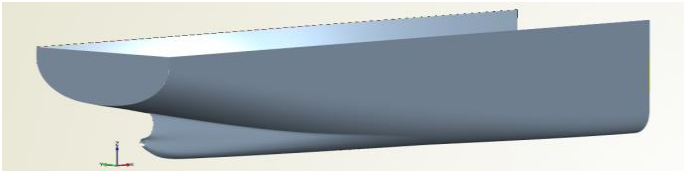

Fig. 3 Modeled aft body

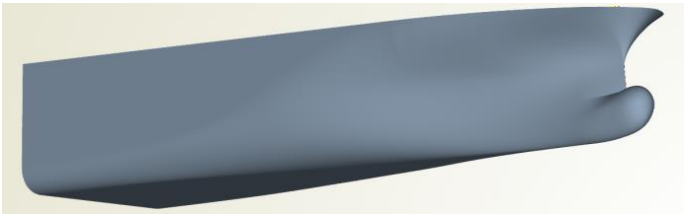

Fig. 4 Modeled fore body

Geometric Model

Modern CAD/CAE software tools are used to generate the parametric ship model, following the principles of a fully parametric design. The model is produced within CAESES/Friendship-Framework (Abt & Harries 2007), and consists of four main parts; the main frame, the aft body, the fore body, and the main deck (Figs. 3 and 4). To sufficiently set up the parametric model, several parameters are defined at this stage. Apart from the main dimensions of the hull, more parameters are created to control various parts of the hull. For example, the bilge height and width, as well as the position of the propeller tube, and the lowest vertical position of the transom are controlled by the parameters.

Lackenby Transformation After the completion of the initial geometric model, a hydrostatic calculation is performed to determine the basic properties of the hull. This is achieved by using an inbuilt hydrostatic connection. After running the connection, the sectional area curve becomes available, and is used as input in the Lackenby transformation. The ultimate purpose is to produce the final hull of the model by adjusting the prismatic coefficient and the longitudinal center of buoyancy (LCB). This process allows shifting sections aft and fore, while fairness optimized B-Splines are utilized. As a result, an adequately faired and smooth hull surface is achieved (Abt & Harries 2007).

Fig. 5 Alternative superstructure models: Model-1 (above) vs. Model-2 (below)

Arrangement of Cargo Spaces & Superstructure Although until this step one hull has been created, from this point onward, two slightly different ship models are designed (Fig. 5). The aspects that differentiate these two designs are the superstructure and, consequently, the internal and external arrangement of the cargo stowage area. As far as the first variant (Model-1) (Fig. 6) is concerned, both the superstructure and the engine room are traditionally positioned at the aft part of the ship. On the other hand, the second variant (Model-2) (Fig. 7) illustrates a more

modern and radical approach, usually found in larger container carriers. In this case, a twin-isle arrangement is employed, with the engine room positioned at the aft part of the hull, whereas the biggest part of the superstructure, which includes the crew accommodation and the wheelhouse, is located at the fore part. The funnel and the stores area are located above the engine room, near the stern of the vessel.

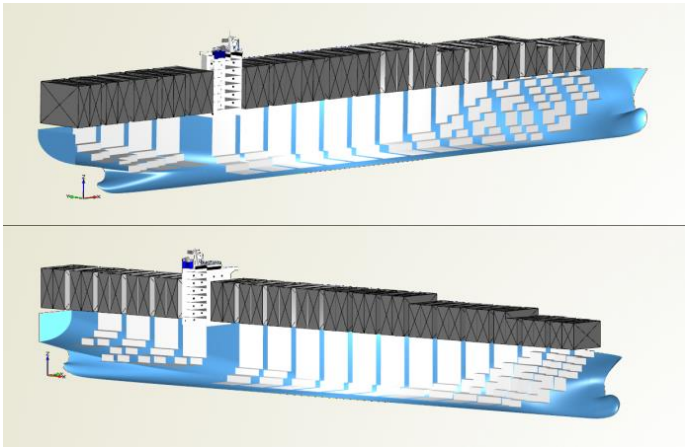

Fig. 6 Superstructure Model-1 cargo storage arrangement

As far as the superstructure is concerned, an inbuilt program is used to create the required surfaces. Parameters such as the number and height of decks, as well as the beam and longitudinal position of the superstructure are defined for the construction of the deckhouse.

The cargo arrangements both below and above the main deck follows afterward. The program responsible for the development of the internal cargo storage arrangement creates the surface on which the TEUs are stored, while monitoring the distance of this inner surface from the outer cell of the hull. This distance in our model is represented by two design variables, the double side and the double bottom parameters.

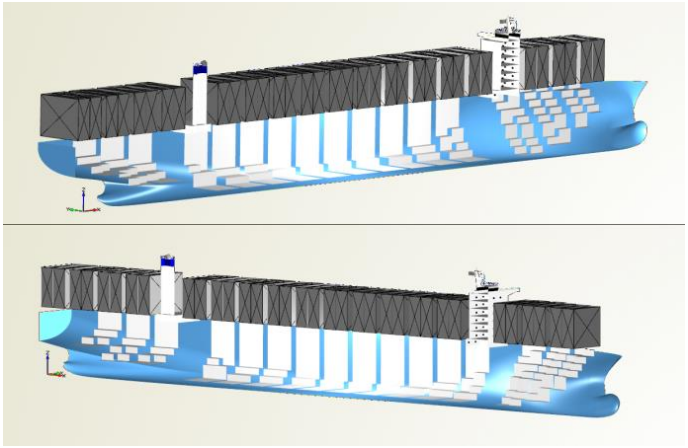

Fig. 7 Superstructure Model-2 cargo storage arrangement

The program responsible for the development of the cargo storage arrangement above the main deck is designed in such a way, so as to take into account the visibility line rule imposed by the IMO. The program automatically takes as input the visibility line defined in our model, thus preventing an excessive vertical stowage of containers above the main deck that would result in disobedience to the rule. In addition, the program follows the deck line and monitors the available space along the beam of the ship to define the proper amount of TEU rows above the main deck.

In both cases, several parameters are set, to define the cargo space, such as the bay spacing and the dimensions of the standardized TEU unit. The result of the computations performed within the program is limited to one bay length, so that the maximum cargo storage capacity is ensured.

Naval Architectural Computations

This part of the project is one of the most time consuming, since all the subsystems that are responsible for the computations regarding the cargo capacity, the deadweight analysis, the propulsion, and resistance of the ship are built at this stage. The computations described below are identical in both variants of the model.

Cargo Capacity After the construction of the geometric model, including the cargo space arrangement and the superstructure, it is possible to continue with the calculation of the actual TEU capacity of the ship. To accomplish this, two programs are created, one for the capacity calculation below the main deck and another one for the capacity calculation above the main deck. Apart from the actual measurement of the TEUs below and above the main deck, these programs are designed to calculate the vertical and longitudinal moments, as well as the vertical and longitudinal centers of gravity, which are used as input in other computations.

Hydrostatics Before proceeding to the remaining computations, a hydrostatic calculation has to be run first. Earlier, the same action took place; however, it was before the final hull was generated. Since its characteristics have changed after the last hydrostatic calculation, a new run is necessary for the following steps of the project.

Resistance Another essential element needed for the design computations is the resistance of the ship. For this purpose, a popular method for the prediction and calculation of the resistance is used, namely the Holtrop and Mennen method (Holtrop & Mennen 1978). Since this method requires numerous calculations for various aspects of the overall resistance, a custom program is developed within the software, requiring a limited amount of input, so as to be as straightforward as possible. The overall resistance is divided into categories as defined by Holtrop and Mennen. At this stage, the service speed of our model is determined, since it is required for the calculations. Taking into account the recent trend of slow steaming, the operational speed is set to 20 knots.

Propulsion The Holtrop and Mennen method includes formulas for the calculation of effective horsepower (EHP) and shaft horsepower (SHP) (Holtrop & Mennen 1978). First, the EHP is

calculated, since the total resistance and the speed of the vessel are known. Having already found the necessary propulsion and efficiency factors from the resistance computations, the calculation of SHP is then possible. The final result is increased by a small percentage to include a bad sea state as well as a fouled hull condition. Next, the estimation of the auxiliary power follows. Finally, the fuel consumption is calculated.

Lightship The next step is to calculate the lightship of the modeled ship. Even though the methods utilized for this step are semiempirical approaches, and thus, an approximation of the exact values, we aim at the most accurate results. In this context, it should be noted that several parameters needed for the computations are derived from applications and detailed calculations performed by the CAESES/Friendship-Framework, such as the enclosed volume of the hull, which is very important for several other calculations. Moreover, the same calculation procedures were applied to a similar 6300-TEU containership, for which we had detailed lightship breakdown and other data. The purpose of this action was to calculate correction factors that would improve the final outcome of our model's lightship computation, since the actual lightship weight and center of gravity of the reference ship were known. Thus, first, all required calculations for the reference ship were performed in Microsoft Excel and a customized code was developed in CAESES/Friendship-Framework, including the same techniques used in the first step, so as to determine the model's lightship characteristics. It should be noted that this feature takes as input the data from the calculations performed in Microsoft Excel, so as to include the correction factors in the model's lightship computation.

The lightship weight is divided into three categories; the steel weight, outfitting weight, and machinery weight. Steel weight is calculated using the Schneekluth and Müller-Köster methods. Outfitting and machinery weights are calculated using existing formulas, taking as input several parameters, such as the main dimensions of the ship, as well as the main engine's power (Papanikolaou 2014).

Finally, longitudinal and vertical centers of gravity are calculated, to be used later at the generation of the examined loading cases.

Deadweight Analysis During this stage, the analysis of the deadweight takes place. For this purpose, some elements have to be outlined, on which most of the related calculations are based. In particular, the range of our vessel is determined at this stage. As mentioned earlier, the route selected for our model is one connecting India with North America. The operational profile of the model is presented in Table 1.

Deadweight is divided into the following categories:

- Diesel oil
- Fuel oil
- Lube oil
- Crew
- Fresh water
- Payload
- Provisions
- Stores

For the calculation of the above weights, data, including the engines' power, fuel consumption, number of crew members and the ship's range are used (Papanikolaou 2014). As in lightship's case, longitudinal and vertical centers of gravity are calculated, to be used at a later stage.

Table 1 Operational profile

Operational speed (knots)	20
One-way route distance (nm)	12,205
Number of ports	18
Average time at port (hours)	15.3
Transit time (days)	63

Tanks Allocation The final design computation that has to be performed is the allocation of the necessary tanks in the model's hull. The tanks created in the model are mainly the ones containing the fuel, diesel and lube oil, as well as the water ballast tanks.

At first, sections which represent the tanks are generated. Afterwards, hydrostatic calculations are performed to determine basic properties of the tanks, such as the volume, weight and the center of gravity.

Design Indicators

In the following section, we define and determine several performance indicators that will be used in the optimization process. The computations described below use information and data derived from the design computations and are identical in both variants of the superstructure model.

EEDI One of the optimization criteria in our project is the minimization of the EEDI. Hence, the calculation of both the attained and the required EEDI values should be included. For this purpose, a customized code is created, which calculates the above values, as described by IMO regulations. On one hand, the attained EEDI value is calculated, based on the following formula:

$$\mathrm{EEDI}_{\mathrm{att}} = \mathrm{a} \cdot \mathrm{b}^{-\mathrm{c}} \cdot \left(1 - \frac{\mathrm{x}}{100}\right)$$

where a and c are equal to 174.22 and 0.201 respectively, according to IMO in case of containerships, b stands for the deadweight of the vessel and x is a reduction factor.

On the other hand, the required EEDI value is calculated using the following formula:

$$\mathrm{EEDI}_{\mathrm{req}} = \frac{(\text{Ship Emissions}) - (\text{Efficiency Technologies})}{(\text{Transport Work})}$$

The ship emissions include that of the main engine, auxiliary engines, as well as the shaft generators, and motor emissions. The efficiency technologies include several arrangements, modifications, or installations to the hull or the propulsion system, which result in increased efficiency. Hence, these technologies should be taken into account in the calculation of the attained EEDI as a reduction factor. Finally, the transport work takes into account the cargo loading of the ship, as well as its service speed (DNV GL 2013; MAN Diesel and Turbo 2015).

Finally, apart from the above values, the custom program calculates the "Attained/Required" EEDI ratio, which is used as a performance indicator during the optimization phase.

RFR The second—and one of the most important—objective function is the RFR of the ship. This value indicates the minimum rate that evens the properly discounted ship's expenses. The main formula used to calculate the RFR is the following:

$$\text{RFR} = \sum_{1}^{N} \left[\frac{\text{PW(Operating cost)} + \text{PW(Ship acquisition cost)}}{\text{(Round Trips)} \cdot \text{(TEUs)}} \right]$$

where PW is the Present Worth of the respective cost. The overall cost is divided into two categories; the operating cost and the ship acquisition cost. The former is mainly based on the running costs of the ship, such as cost for the fuel, crew, stores, maintenance, insurance, administration, and port costs. As far as the fuel cost is concerned, a review is made first, so as to identify the HFO and MDO costs. Then, taking into account the route length and the fuel consumption of the model, the total fuel cost is reckoned. As far as the ship acquisition cost is concerned, to perform the calculations, several data are used as input, including the steel mass of the vessel, cost of steel, discount rate, operation time, main dimensions, and engines' power.

Of course, as in previous cases, a custom program is defined, so that the calculations are performed automatically whenever a parameter changes.

Trim & Stability One of the most important innovation elements in our model is the control of trim and stability, while optimizing for maximum number of containers on deck and minimum carried ballast. This step is anyway essential for the implementation of the next one, namely the generation of the loading cases.

Within this software module, essential ship hydrostatic and stability parameters are determined, such as the values of the restoring arm lever GZ-ϕ curve, the trim of the ship, as well as the vertical center of mass (gravity) KG and longitudinal center of mass (gravity) LCG values that will be used in the loading cases computation. The stability is evaluated by assuming a homogenous stow. The assessment of the initial and large angle stability of the vessel is undertaken for common type loading conditions in accordance with the IMO A.749/A.167 intact stability criteria. The code used in this project generates the GZ-ϕ curve, by running several hydrostatic computations at various heeling angle values. A continuous check is performed, to ensure that the model complies with the IMO intact stability criteria. If the latter is not the case, the stowage of cargo, ballast and fuel, along with the associated KG and LCG values are modified and the whole process is repeated, until the criteria are met.

The ultimate goal of this iterative procedure is to minimize the amount of carried water ballast and identify "zero ballast" loading conditions. During this procedure, the payload weight, calculated based on the homogenous weight per TEU, as well as its vertical center of gravity are taken into account.

Loading Cases The last computation required is the generation of the loading conditions. Two different conditions are investigated in this project. Both of them require several parameters and elements determined in previous stages. These parameters consist of various weight groups, as well as their longitudinal and vertical centers of gravity which represent the data used as input in this computation. These groups include the displacement, the lightship, the payload, divided into the below and above main deck TEUs, the consumables, and the water ballast. As far as the water ballast is concerned, several groups are defined, to fill only the minimum required space with sea water. For instance, only the fore peak tank may be filled with water ballast, or in case more ballast is needed, the bilge or double bottom tanks may be used.

The loading conditions investigated in this project are the maximum TEU capacity and the zero ballast conditions. As far as the former condition is concerned, the main objective is to maximize the cargo capacity, taking into account the IMO rules. However, it affects the homogeneous weight per container. On the other hand, the latter condition is defined as a condition where no water ballast is loaded for stability reasons, with the exception of some limited water ballast in the aft and fore peak tanks, for trim balance. Hence, the number of TEUs aboard the ship is restricted due to limitations described in the trim and stability computation stage. The objective in this case is the maximization of the number of loaded TEUs.

Port Efficiency Indicators At this point, every necessary computation has been described. However, since port efficiency is included in the optimization objectives, a parameter must be defined. Having access to a detailed calculation of the TEU stowage below and above the main deck, a parameter called "Stowage ratio" is created within CAESES/Friendship-Framework, which takes as input the number of containers stacked above and below the main deck, calculated in a previous computation. It can be understood that the higher the ratio, the more efficient is the ship.

Zero Ballast Water Indicators As far as the zero ballast condition is concerned, a performance indicator, which is also one of the objectives of the optimization procedure, is defined at this stage. Instead of using the actual TEU capacity of the zero ballast condition, a parameter called "Capacity ratio" is used. This ratio is defined by dividing the number of containers the ship can transport while in zero ballast to the maximum TEU capacity of the ship. As in stowage ratio's case, the higher the capacity ratio, the more competitive is the vessel.

Design Exploration

Before proceeding to the formal optimization rounds, a design of experiment (DoE) is conducted first. This process will allow us to examine the design space and the response of several parameters to the change of the model's main characteristics. The algorithm utilized in this phase is the Sobol algorithm, a quasirandom sequence which secures the overall coverage of the design space, whereas the overlapping of previous set of sequences is avoided (Azmin & Stobart 2015). Through the DoE, the investigation of the feasibility boundaries is ultimately achieved, allowing us to detect the trends of the design variables in regard to the optimization objectives. In our case, the design engine is assigned to create 500 variants of our model. Since two versions—Model-1 and Model-2—are built, the DoE is conducted twice, once for each variant. To start the DoE, the design variables and the constraints need to be defined first (Tables 2 and 3). At this point, no objectives need to be determined, since only the feasibility boundaries are investigated. However, several parameters are evaluated through this process.

Table 2 Design variables

Design variable	Min. value	Max. value
Bays	18	20
Rows	14	18
Tiers in hold	8	10
Tiers on deck	6	8
Double bottom (m)	1.9	2.6
Double side (m)	2.0	3.0
Variation of prismatic coefficient ΔC_P	-0.06	0.06
Variation of longitudinal center of buoyancy ΔLCB	-0.026	0.026

Table 3 Design constraints

Constraint	Value
"Attained/Required" EEDI	≤ 1
GZ area (0^o-30^o)	≥ 0.055 m-rad
GZ area (0^o-40^o)	≥ 0.09 m-rad
GZ area (30^o-40^o)	≥ 0.03 m-rad
Initial metacentric height (GM)	≥ 0.15 m
Angle at GZ_{max}	$\geq 30^o$
GZ_{max} value	≥ 0.2 m
Homo weight/TEU (max.)	≥ 6 t
Homo weight/TEU (Zero Ballast condition)	≥ 7 t
Trim at FLD (Full Load Departure condition)	$\leq 0.5\%$ L_{BP}

Moreover, the constraints are set, so as to have a clear view of which of the subsequent variants violate several criteria that must be met. For instance, various stability criteria are included in the constraints. In case one of them is violated, the variant cannot be considered as a satisfactory alternative to the base model, even if some of the objectives are improved.

When the run ends, a wide variety of results are displayed, which inform us about the design space. It is worth mentioning that the TEU capacity of the model is not constrained, thus the maximum and minimum number of TEU capacity of the variants is not limited to the 6000–7000 area.

Multi-Objective Optimization

The last step to complete our work is to run the formal optimization rounds. To achieve that, the Non-dominated Sorting Genetic Algorithm II (NSGA-II) is utilized, a genetic algorithm which produces satisfactory results (Deb et al. 2002). To ensure that the optimal design is found, two rounds are run for every version of our model. In particular, during each run, five generations are created, having a population size of 50, each. Since the DoE provided fairly decent results, the same baseline model is used for the first round. The best variant produced during the first round is then used as the baseline model for the second and final optimization round. In addition, the design variable extents remain the same, as the design space seems to be well defined. As far as the constraints are concerned, apart from the ones defined in the previous stage, two additional constraints are set to delimit the maximum TEU capacity of the ship variants. Therefore, an upper (7000 TEUs) and lower (6000 TEUs) limit is defined. Unlike the previous phase, in this case, apart from the evaluation of various parameters of the model, several objectives are defined:

- Minimization of the RFR
- Maximization of the Capacity ratio
- Minimization of the EEDI
- Maximization of the Stowage ratio
- Minimization of the overall ship resistance

Table 4 Case scenarios

Objective	Scenario 1 (%)	Scenario 2 (%)	Scenario 3 (%)
RFR	20	50	20
Capacity ratio	20	20	50
EEDI	20	10	10
Stowage ratio	20	10	10
Total ship resistance	20	10	10

The results of a multidisciplinary optimization procedure might not provide a straightforward solution to a problem. Although the algorithm used for the optimization provides some improved designs, it is not always clear which one is the best. For this reason, several case scenarios are created, so as to determine the optimal of the top solutions to the problem. In our project, three distinctive scenarios are defined, where the significance of each objective is acknowledged differently by assigning specific "weights" following the utility functions technique of decision making theory (Table 4). In scenario 1, all five explored objectives are considered to be equally important; hence each one is assigned a weight of 20%. On the other hand, in scenarios 2 and 3, the RFR and capacity ratio are chosen to be more significant for the decision maker (designer, operator) by assigning to them a weight of 50% and 20% in both cases, whereas the rest of the objectives are assigned a weight of 10%.

After obtaining the results of each run, the data are normalized according to the scenarios. Afterward, the normalized data are ranked to find the optimal variant of our model. In most cases, a specific variant dominates in every scenario. In this case, the selection of the optimal solution is unambiguous. However, if the process does not lead to a clear-cut result, the decision lies with the designer. As far as our project is concerned, the normalization of the data provided concrete results. The above procedure is utilized both after the end of the first optimization run to determine the new, improved baseline model for the second run, and after the end of the final run, so as to determine the optimal final design.

DISCUSSION OF RESULTS

Base Model

Before proceeding to the actual results, some essential information about the base model is presented, to have a clear perspective of the initial hull (Tables 5 and 6).

Table 5 Base model design variable values

Design variable	Base model value
Bays	19
Rows	16
Tiers in hold	9
Tiers on deck	6
Double bottom (m)	2.0
Double side (m)	2.1
Δc_P	-0.01125
ΔLCB	-0.00375

Table 6 Base model objective values

Objective	Model-1	Model-2
RFR ($/TEU)	634.68	644.10
Capacity ratio	0.5193	0.5292
EEDI	9.21	9.20
Stowage ratio	0.9451	1.0145
R_T (KN) Total Resistance	1635	1635

Design of Experiments

The DoE phase enables the exploration of the huge design space, which is impossible in traditional ship design procedures. The following observations can be made. As far as the correlation between the number of bays and the number of TEUs is concerned, it is evident that as the former increases, the latter also gets higher. The same behavior can be observed as to the dependency on the number of rows (Figs. 8 and 9).

Furthermore, since the formula used to calculate the attained EEDI contains the transport work, which is relative to the deadweight of the vessel, it is clear that changes in the displacement of the model result in variation of the attained EEDI. An increase in the displacement of the model normally leads to an increase of deadweight. Since the deadweight is inversely proportional to the attained EEDI, as the displacement of the model increments, the index trivially declines, which is anyway expected by the economy of scale (Fig. 10).

Finally, as far as the dependency of EEDI and RFR on the displacement and TEU capacity is concerned, it is evident that both EEDI and RFR decrease, with an increase in ship size and capacity, which is a clear indication of the economy of scale. Furthermore, there is a good correlation in the behavior of EEDI and RFR with respect to their dependence on ship size, which can be readily explained by the nature/definition of these two ship performance indicators (Fig. 11).

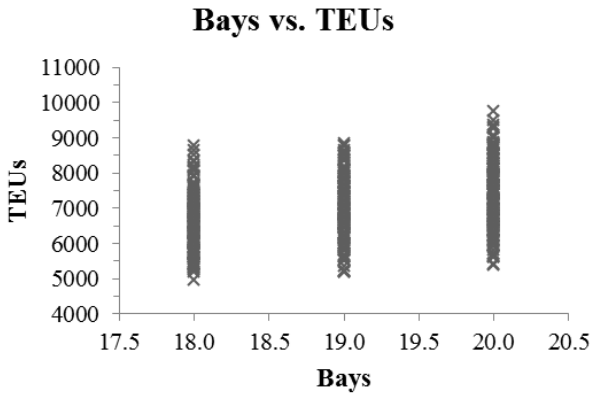

Fig. 8 Variation of TEU capacity with number of bays

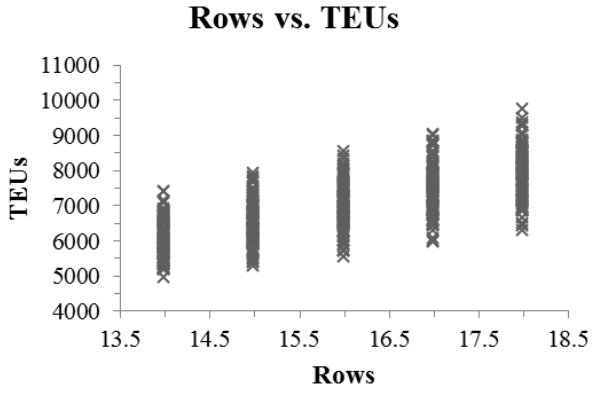

Fig. 9 Variation of TEU capacity with number of rows

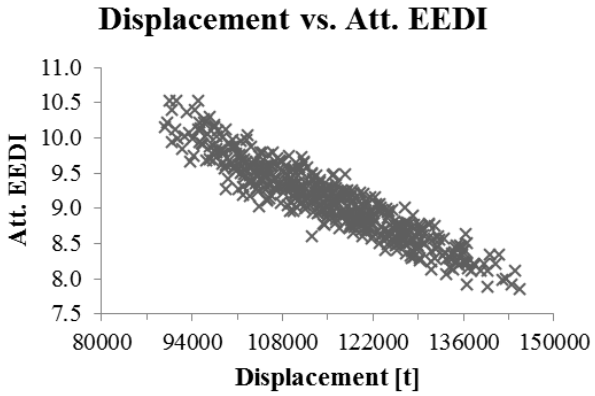

Fig. 10 Displacement vs. Attained EEDI

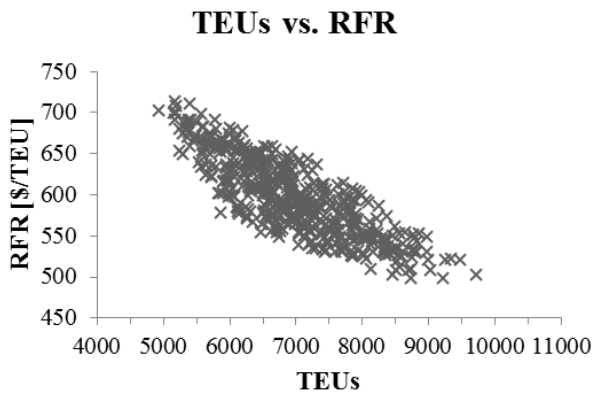

Fig. 11 TEU capacity vs. RFR

Multi-Objective Optimization

Model-1 As far as Model-1 variant is concerned, after the two NSGA-II rounds and the evaluation of both rounds' results, we concluded that the best design, namely Des0129, was produced during the first round. Below, some principal information of Des0129 can be found (Fig. 12, Tables 7 and 8).

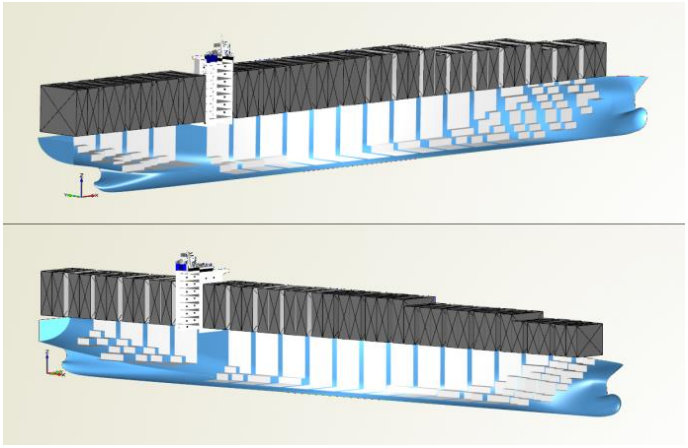

Fig. 12 Des0129 model

As far as the values of the attained EEDI in respect to the number of bays are concerned, low values in variants having 20 bays are noticeable, whereas in case of 18 and 19 bays, the range of EEDI values is bigger, running from around 8.25 to 10. A decrease in the attained EEDI can be noticed between the base and the improved model (Fig. 13).

Table 7 Des0129 design variable values

Design variable	Des0129
Bays	20
Rows	16
Tiers in hold	8
Tiers on deck	7
Double bottom (m)	2.00
Double side (m)	2.63
Δc_P	0.02416
ΔLCB	0.00102

Table 8 Des0129 objective values

Objective	Des0129
RFR ($/TEU)	579.99
Capacity ratio	0.5179
EEDI	8.58
Stowage ratio	1.3191
R_T (KN)	1688

In case of the two examined ratios—stowage and capacity—high values for both ratios are desired. However, a decrease in the stowage ratio is observed, as the capacity ratio rises (Fig. 14). However, a few variants deviate from this behavior and achieve high stowage and capacity ratios. Among these designs is Des0129. All in all, between the base and the improved model, we notice an impressive increase in the stowage ratio, whereas the capacity ratio remains nearly the same in both cases.

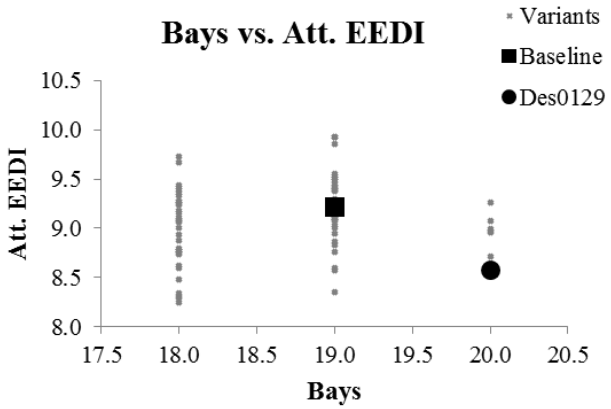

Fig. 13 Number of bays vs. Attained EEDI

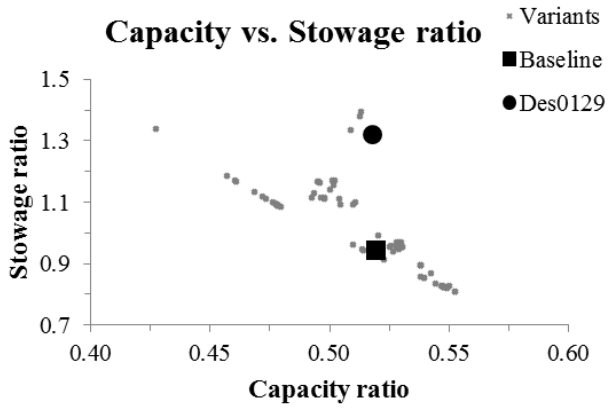

Fig. 14 Capacity vs. Stowage ratio

As far as the relationship between RFR and the stowage ratio is concerned, an optimal solution would be characterized by a low RFR value and a high stowage ratio. Most of the design variants range between 620 and 675 $/TEU as far as the RFR is concerned, whereas their stowage ratios range between 0.8 and 1.2. However, a few generated designs present lower RFR values and slightly higher stowage ratios. Des0129 is located in this area, achieving both a satisfactory freight rate and a high stowage ratio (Fig. 15).

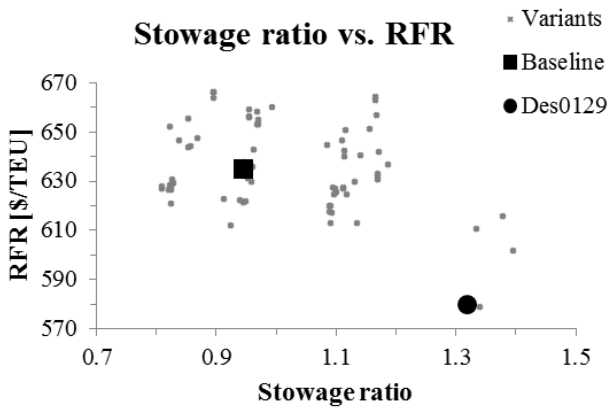

Fig. 15 Stowage ratio vs. RFR

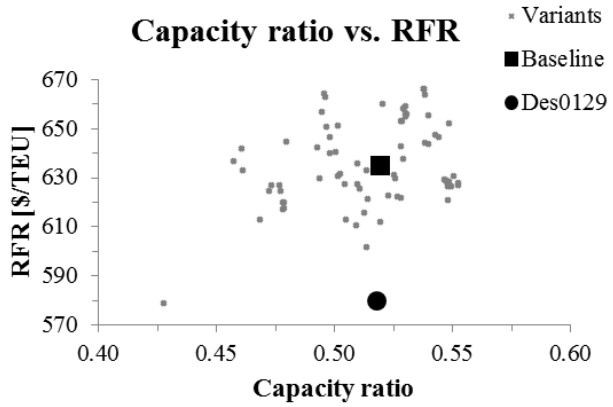

Fig. 16 Capacity ratio vs. RFR

Finally, the relation between the RFR and the capacity ratio is available. The optimal variant is located far from most of the generated designs in the diagram, along with another variant. Both of these designs feature a low freight rate. However, Des0129 features an adequate capacity ratio, which is almost the same as that of our base model (Fig. 16).

To select the optimal design, namely Des0129, a decision making process takes place. The results from the optimization runs are normalized and evaluated, taking into account the assumed scenarios.

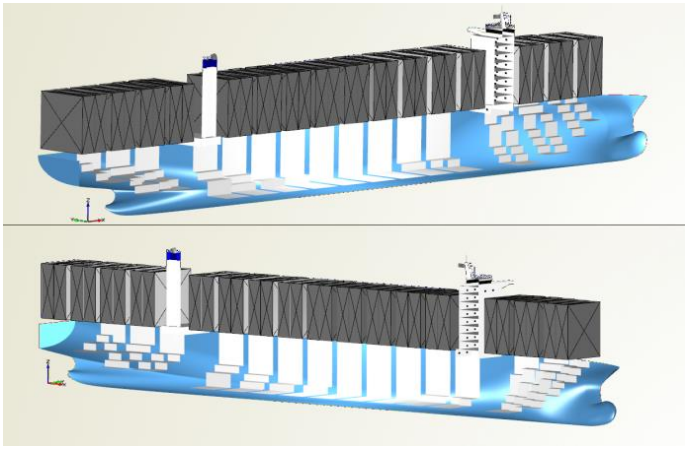

Fig. 17 Des0080 model

Table 9 Des0080 design variable values

Design variable	Des0080
Bays	18
Rows	17
Tiers in hold	8
Tiers on deck	8
Double bottom (m)	2.52
Double side (m)	2.69
Δc_P	-0.02636
ΔLCB	0.01825

Table 10 Des0080 objective values

Objective	Des0080
RFR ($/TEU)	562.93
Capacity ratio	0.5344
EEDI	8.98
Stowage ratio	1.6250
R_T (KN)	1582

Model-2 Following the same steps as in Model-1's case, after the optimization rounds, an optimal variant was identified, namely Des0080. Below, some principal information of Des0080 can be found (Fig. 17, Tables 9 and 10).

Unlike Model-1, Des0080 features one bay less than the initial model. Looking at the EEDI vs. Bays diagram, we see a 2% decrease in the attained EEDI value. Moreover, we can observe a steady decline in the EEDI values as the number of bays increases (Fig. 18).

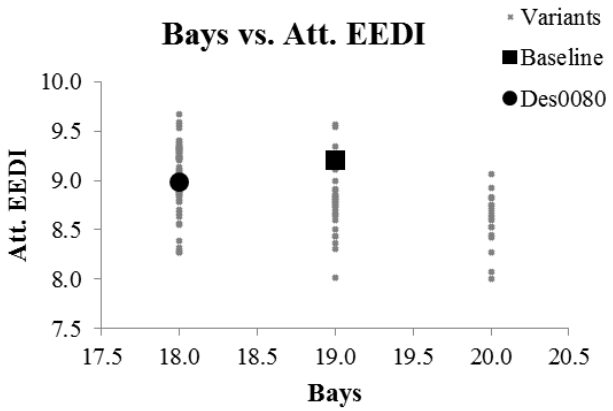

Fig. 18 Number of bays vs. Attained EEDI

As far as the relation between the stowage and capacity ratios is concerned, the situation resembles Model-1's case (Fig. 19). A general decline in capacity ratio can be observed, as the stowage ratio rises. However, our improved model, along with a couple of generated variants, seems to achieve high values in both ratios. Des0080 in particular, manages to increase its capacity ratio by little, while boosting its stowage ratio by more than 60%, compared to the baseline model.

The correlation between RFR and stowage ratio is investigated next (Fig. 20). Looking at the position of the design variants in the diagram, it becomes fathomable that as the ratio values rise,

the RFR values descend. Des0080 is positioned far from most of the variants, including the base model, achieving both the highest stowage ratio and the lowest freight rate.

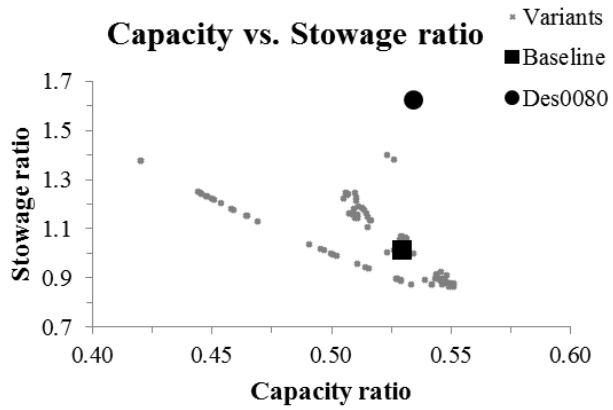

Fig. 19 Capacity ratio vs. Stowage ratio

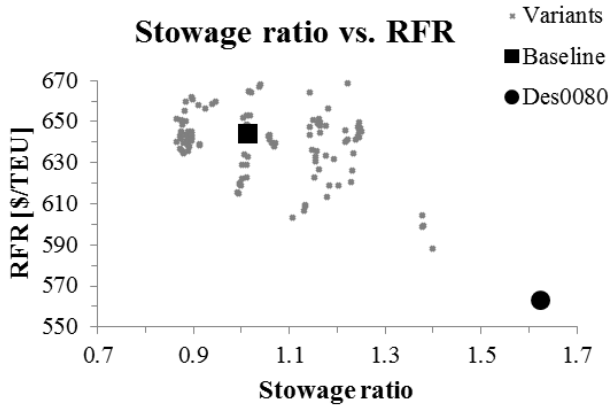

Fig. 20 Stowage ratio vs. RFR

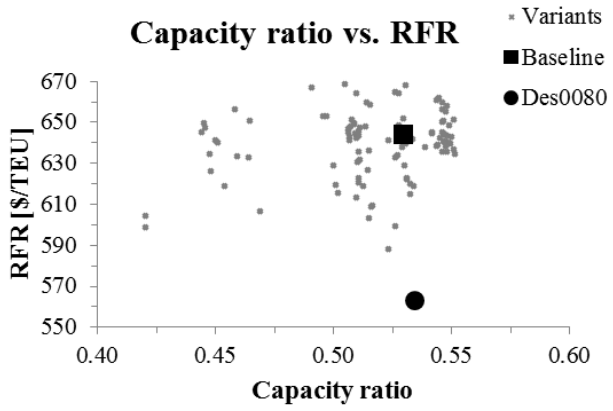

Fig. 21 Capacity ratio vs. RFR

Finally, the relation between the RFR and the capacity ratio is examined (Fig. 21). Most of the design variants are characterized by adequate capacity ratios; however, the freight rate is kept relatively high. Nevertheless, Des0080 manages to combine satisfactory results in both objectives. In particular, the RFR value sees a sharp decrease of around 12.5%, compared to the base model.

In Figs. 19–21, a few outliers can be spotted, which show very favorable results for the capacity and stowage ratios, as well as for the RFR. Des0080 is among them. Analyzing the detailed results of the optimization, we observe that these "outliers" are the only successful (in the sense of passing all set design constraints) designs featuring seven or eight tiers of containers above the main deck. Because of stability reasons, most of the other successful design variants can carry only up to six tiers of containers above the main deck. The extra one or two tiers found in these outliers offer the advantage of an increased stowage and capacity ratio, as well as a reduced RFR, due to the higher total number of TEUs carried on board. It should also be mentioned that these designs are also characterized by the low number of tiers below the main deck, down to eight, compared to 10, which can be found in the other successful variants.

Optimal Design Selection Comparing the identified most favorable designs Des0129 and Des0080 we note the following.

Table 11 Des0129 vs. Des0080 principal data

Data	Des0129	Des0080
Length between perpendiculars (L_{BP}) (m)	305.53	276.00
Beam (B) (m)	39.01	41.45
Depth (D) (m)	21.69	22.21
Block coefficient (C_B)	0.7269	0.6859
Midship coefficient (C_M)	0.9821	0.9832
Prismatic coefficient (C_P)	0.7401	0.6976
Displacement (t)	124,337	112,611
Deadweight (t)	97,241	88,683
Lightship (t)	27,096	23,928

Table 12 Des0129 vs. Des0080 objective values

Objective	Des0129	Des0080
RFR ($/TEU)	579.99	562.93
Capacity ratio	0.5179	0.5344
EEDI	8.58	8.98
Stowage ratio	1.3191	1.6250
R_T (KN)	1688	1582

First, a comparison regarding the main characteristics of Des0129 and Des0080 is made. The main differences between the two variants can be spotted in their length between perpendiculars (L_{BP}) and beam values. In particular, Des0080 features a smaller L_{BP}, whereas its one extra row produces a wider hull, compared to Des0129. The result is a much lower lightship weight, as far as Des0080 is concerned. Moreover, the deadweight/displacement ratio is higher in Des0080 than in Des0129. In addition, the block coefficient (C_B) value of Des0080 is considerably lower than Des0129's one, even though this variant has a larger beam. These observations help us to understand why Des0080 achieves both a lower freight rate and a lower total resistance (Tables 11 and 12).

The information provided above is sufficient for us to proceed to the decision making process. Since Des0080 outranks Des0129 in every objective, but for EEDI (which is anyway below required regulatory index), it is rational to declare Des0080 as the

Table 13 Overall comparison

Data	Des0080	Ship 1	Ship 2	Ship 3
L_{BP} (m)	276.00	287.00	306.58	286.00
B (m)	41.45	40.00	40.06	42.84
D (m)	22.21	23.90	24.20	24.50
Displacement (t)	112,611	110,715	115,832	111,270
Deadweight (t)	88,683	82,275	87,534	88,700
Lightship (t)	23,928	28,440	28,298	22,570
Maximum TEU capacity	6,980	6,208	6,478	6,802
RFR ($/TEU)	562.93	666.37	667.05	644.37
EEDI	8.98	10.06	9.57	9.36
R_T (KN)	1582	1603	1620	1588
Main Engine Power ($P_{B,ME}$) (KW)	26,829	27,882	28,242	27,987

best design of the optimization process carried out in this project. To further elaborate on the selection of Des0080 as the optimal variant, a detailed comparison with some of the existing vessels that were used as input during the creation of the parametric model is made (Table 13). It should be mentioned that the calculations of both the RFR and the EEDI of the existing containerships—ships 1, 2, and 3—were performed using the same methods as in our model in Friendship-Framework, so as to be fair in this procedure. Moreover, every ship is supposed to operate at 20 knots, in order for their required main engine power to be more or less the same and consequently, the comparison to be realistic.

All in all, the superiority of Des0080 is evident in the comparison table. At similar dimensions, Des0080 is able to carry the highest number of TEUs. Des0080's RFR value is considerably lower than the rest of the ships. The same stands for the attained EEDI value, where Des0080 achieves the lowest number. Furthermore, the overall resistance of Des0080 is lower than the one of the existing ships, but it is worth mentioning that ship 3 achieves a low overall resistance as well.

Table 14 Model-2 vs. Des0080

Data	Model-2	Des0080	Difference
Bays	19	18	-1
Rows	16	17	+1
Tiers in hold	9	8	-1
Tiers on deck	6	8	+2
Double bottom (m)	2.00	2.52	+0.52
Double side (m)	2.10	2.69	+0.59
R_T (KN)	1635	1582	-3.24%
Maximum TEU capacity	6394	6980	+9.16%
Zero Ballast TEU capacity	3384	3730	+10.22%
Capacity ratio	0.5292	0.5344	+0.98%
Stowage ratio	1.0145	1.6250	+60.17%
RFR ($/TEU)	644.10	562.93	-12.60%
EEDI	9.20	8.98	-2.39%

Apart from the freight rate and the EEDI, various differences can be spotted in the main dimensions of the ships. Des0080 features the lowest length and depth, whereas its beam is the second biggest. The twin-isle arrangement, however, offers the advantage of an increased number of TEUs stored above the main deck, since the visibility line rule is practically not a restriction in this configuration, contrary to the rest of the ships, which feature a traditional arrangement.

Finally, a one-to-one comparison between the initial and the improved design is made, to show the percentage differences in several elements (Table 14). Overall, the improvement of the initial containership design is obvious. Des0080 manages to perform much better, reducing the RFR by 12.6% and the attained EEDI by 2.39%. Moreover, the capacity ratio is increased, which means that the zero ballast TEU capacity is improved, while at the same time, more TEUs can be stored above the main deck, simplifying the cargo loading and unloading process.

SUMMARY & CONCLUDING REMARKS

Through the work presented in this paper, the advantages of the utilization of modern design optimization in the shipbuilding industry are demonstrated. By incorporating this type of parametric optimization process in the early stages of ship design, a much improved design can be produced, providing numerous benefits to a potential builder and end user (shipowner). Furthermore, it is demonstrated that using modern CAD/CAE systems, it is possible to explore the huge design space with little effort, while generating excellent/partly innovative results within very short lead times. The presented methodology and the implemented CAD system allows the integration of more advanced tools for the improved modeling of, e.g., the ship's hydrodynamics or the ship's strength (Sames et al. 2011). The areas of optimization are of course not limited to the objectives examined in this project. Aspects such as structural strength or seakeeping can become main objectives of design optimization as well, as necessary, allowing naval architects to achieve a greater degree of holism in the design process (Papanikolaou 2010).

As far as the results of the current application are concerned, some general observations can be made and conclusions drawn.

First, the consideration of twin-isle arrangements for such containership sizes seems to be attractive, as the resulting best variant proved to feature such a configuration. This may be justified,

also, by other reasoning and is confirmed in practice for the larger capacity containerships. In addition, it is worth mentioning that shorter and wider designs prove to be more cost-efficient than longer and narrower ones. A decrease in ship length can lead to a much lower lightship value, thus increasing the deadweight of the ship and, consequently, its overall cost-efficiency. Nevertheless, wider designs may be more prone to increased transverse accelerations in seaways, that are herein partly controlled by an upper limit for ship's metacentric height GM. Finally, it should be noted that the wider variant promoted herein disposes some additional unique hull form features; among them, we note its unique midship section, which has an elliptic bilge, following previous work of the Ship Design Laboratory (Koutroukis 2012). This extended bilge, which results "naturally" by the employed hull form design optimization procedure, exploits the geometrical properties of the ellipse and allows decreasing the wetted surface of the ship, whereas the displacement volume is not equally decreased and almost kept constant. The parameters used to control this surface are herein the flat of bottom extent and the flat of side extent. Details may be found in other publications of the CONTiOPT project team (CONTiOPT 2012–2014; Köpke et al. 2014; Koutroukis et al. 2013).

The methodology presented in this study can be also applied to other containership sizes (Koutroukis 2012; Soultanias 2014) and ship types. More phases of the ship's life cycle can be integrated to future studies, resulting in more comprehensive holistic ship design investigations (Papanikolaou 2010).

ACKNOWLEDGEMENTS

The reported research was conducted in the frame of the bilateral JIP project CONTiOPT (2012–2014), which has been financially supported by Germanischer Lloyd, Hamburg. The authors would like to express their sincere gratitude to the following people for their manifold support in this project: Dr. Pierre Sames (DNV GL), Dr. Stefan Harries (Friendship Systems), Martin Köpke (HAPAG Lloyd, former GL), George Koutroukis (former NTUA-SDL), Lampros Nikolopoulos (STARBULK, former NTUA-SDL), Elias Soultanias (NTUA-SDL), and Aimilia Alisafaki (NTUA-SDL).

REFERENCES

ABT, C. AND HARRIES, S. 2007 Hull variation and improvement using the generalized Lackenby method of the friendship-framework, The Naval Architect, pp. 166–167.

BROWN, A. AND SALCEDO, J. 2003 Multiple-objective optimization in naval ship design, Naval Engineers Journal, 115, 4, 49–62.

CAMPANA, E., LIUZZI, G., LUCIDI, S., PERI, D., PICCIALLI, V., AND PINTO, A. 2009 New global optimization methods for ship design problems, Optimization and Engineering, 10, 533–555.

CLARKSON RESEARCH SERVICES. 2014 Container Intelligence Monthly. June 2014.

CONTIOPT 2012–2014 Formal safety assessment and optimization of container ships, Collaborative RTD project of Germanischer Lloyd, NTUA-Ship Design Laboratory and Friendship Systems. Hamburg-Athens-Potsdam.

DEB, K., PRATAP, A., AGARWAL, S., AND MEYARIVAN, T. 2002 A fast and elitist multi-objective genetic algorithm: NSGA-II, IEEE Transactions on Evolutionary Computation, 6, 2, 182–197.

DNV, GL. 2013 Guidelines for Determination of Energy Efficiency Design Index, Rules for Classification and Construction, Chapter VI: Additional Rules and Guidelines, 13: Energy Efficiency. Publ. by Germanischer Lloyd SE. Hamburg.

HOLTROP, J. AND MENNEN, G. G. J. 1978 An approximate power prediction method, International Shipbuilding Progress, 25, 166–170.

IMO MEPC 64/4/13. 2012 Consideration of the energy efficiency design index for new ships—minimum propulsion power to maintain the maneuverability in adverse conditions, Submitted by IACS, BIMCO, INTERCARGO, INTERTANKO, and OCIMF, International Maritime Organisation. London.

IMO RESOLUTION MEPC.212(63). 2012 2012 Guidelines on the method of calculation of the attained energy efficiency design index (EEDI) for new ships, adopted on March 2, 2012, MEPC 63/23, ANNEX 8.

KÖPKE, M., PAPANIKOLAOU, A., HARRIES, S., NIKOLOPOULOS, L., AND SAMES, P. 2014 CONTiOPT—holistic optimization of a high efficiency and low emission container ship, Proceedings, 3rd European Transport Research Arena, TRA2014, April 14–17, Paris, France.

KOUTROUKIS, G. L. 2012 Parametric design and multi-objective optimization study of an ellipsoidal containership, Diploma-Master thesis, National Technical University of Athens, Ship Design Laboratory.

KOUTROUKIS, G. L., PAPANIKOLAOU, A., NIKOLOPOULOS, L., SAMES, P., AND KÖPKE, M. 2013 Multi-objective optimization of container ship design, Proceedings, The 15th International Congress of the International Maritime Association of the Mediterranean (IMAM 2013), October 14–17, A Coruña, Spain.

MAN DIESEL AND TURBO. 2015 Energy Efficiency Design Index. MAN Diesel and Turbo. Augsburg, Germany. Available at: https://marine.man.eu/docs/librariesprovider6/4-Stroke-Engines/eedi-energy-efficiency-design-index.pdf?sfvrsn=6 [Accessed March 2015].

MIZINE, I. AND WINTERSTEEN, B. 2010 Multi-level hierarchical system approach in computerized ship design, Proceed-

ings, The 9th International Conference on Computer and IT Applications in the Maritime Industries (COMPIT ’10), April 12–14, Gubbio, Italy.

MOHD AZMIN, F. AND STOBART, R. 2015 Benefiting from Sobol Sequences Experiment Design Type for Model-based Calibration, SAE Technical Paper 2015-01-1640.

NOTTEBOOM, T. AND CARRIOU, P. 2009 Fuel surcharge practices of container shipping lines: is it about cost recovery or revenue making? Proceedings, The 2009 International Association of Maritime Economists (IAME) Conference, June 24–26, Copenhagen, Denmark.

PAPANIKOLAOU, A. 2010 Holistic ship design optimization, Computer-Aided Design, 42, 11, 1028–1044.

PAPANIKOLAOU, A. 2014 Ship Design: Methodologies of Preliminary Design, Netherlands: Springer. ISBN 978-94-017-8750-5.

PLATTS. 2015 Bunkerworld. Available at: http://www.bunkerworld.com/prices. [Accessed March 2015].

PRIFTIS, A. 2015 Parametric design and multi-objective optimization of a 6,500 TEU container ship, Diploma-Master thesis, National Technical University of Athens, Ship Design Laboratory.

SAMES, P., PAPANIKOLAOU, A., HARRIES, S., COYNE, P., ZARAPHONITIS, G., AND TILLIG, F. 2011 BEST plus—better economics with safer tankers, Proceedings, The Annual Meeting of the Society of Naval Architect and Marine Engineers (SNAME), November 16–18, Houston, TX.

SOULTANIAS, I. 2014 Parametric ship design and holistic design optimization of a 9K TEU container carrier, Diploma-Master thesis, National Technical University of Athens, Ship Design Laboratory.

TOZER, D. 2008 Container Ship Speed Matters, London UK: Lloyd’s Register Group.

UNCTAD. 2014 Review of maritime transport 2014, New York and Geneva: United Nations, Available at: http://unctad.org/en/PublicationsLibrary/rmt2014_en.pdf.

WHITE, R. 2010 Ocean shipping lines cut speed to save fuel costs, Los Angeles, CA: Los Angeles Times. July 31 2010. Available at: http://articles.latimes.com/2010/jul/31/business/la-fi-slow-sailing-20100731.

WORLD SHIPPING COUNCIL. 2015 Trade routes for year 2013. Available at: http://www.worldshipping.org/about-the-industry/global-trade/trade-routes. [Accessed March 2015].